Molecular composition and possible transformations of labile soil organic matter fractions in Mediterranean arable soils: relevance and implications

Hamada Abdelrahman [a *], Diana Hofmann [b], Rachel L. Sleighter [c], Daniel C. Olk [d], Anne E. Berns [b], Teodoro Miano [e], Sabry M. Shaheen [f, g, h], Claudio Cocozza [e]

[a] Cairo University, Faculty of Agriculture, Soil Science Dept., Giza 12613, Egypt

[b] Forschungszentrum Jülich GmbH, Institute of Bio- and Geosciences, IBG-3: Agrosphere, Jülich, Germany

[c] FBSciences, Inc., Research and Development, Norfolk, VA, USA

[d] USDA–ARS, National Laboratory for Agriculture and the Environment, Ames, IA, USA

[e] DiSSPA–Università degli Studi di Bari "Aldo Moro", Bari, Italy

[f] University of Wuppertal, School of Architecture and Civil Engineering, Institute of Foundation Engineering, Water- and Waste-Management, Laboratory of Soil- and Groundwater-Management, Pauluskirchstraße 7, 42285 Wuppertal, Germany

[g] King Abdulaziz University, Faculty of Meteorology, Environment, and Arid Land Agriculture, Department of Arid Land Agriculture, 21589 Jeddah, Saudi Arabia

[h] University of Kafrelsheikh, Faculty of Agriculture, Department of Soil and Water Sciences, 33516, Kafr El-Sheikh, Egypt

[*] Corresponding Author:

Hamada Abdelrahman, hamada@cu.edu.eg, ORCiD: 0000-0002-6069-7239

Abstract

With the increased global interest in sequestering carbon in soil, it is necessary to understand the composition of different pools of soil organic matter (SOM) that cycle over suitably short timeframes. To explore in detail the chemical composition of agroecologically relevant yet distinct fractions of SOM, the light fraction of SOM (LFOM), the 53-µm particulate organic matter (POM), and the mobile humic acid (MHA) fractions were sequentially extracted from agricultural soils and characterized using both ^{13}C cross polarization magic angle spinning nuclear magnetic resonance (CPMAS NMR) spectroscopy and also Fourier transform ion cyclotron resonance mass spectrometry (FT-ICR-MS). The NMR results showed a decrease in the O-alkyl C region assigned to carbohydrates (51–110 ppm) and an increase in the aromatic region (111–161 ppm) proceeding from the LFOM to the POM and then to the MHA fraction. Similarly, based on the thousands of molecular formulae assigned to the peaks detected by FT-ICR-MS, condensed hydrocarbons were dominant only in the MHA, while aliphatic formulae were abundant in the POM and LFOM fractions. The molecular formulae of the LFOM and POM were mainly grouped in the high H/C lipid-like and aliphatic space, whereas a portion of the MHA compounds showed an extremely high (17–33, average of 25) double bond equivalent (DBE) values, corresponding to low H/C values of 0.3–0.6, representative of condensed hydrocarbons. The labile components appeared most pronounced in the POM (93% of formulae have H/C$\geq$1.5) similar to the LFOM (89% of formulae have H/C$\geq$1.5) but in contrast to the MHA (74% of formulae have H/C$\geq$1.5). The presence of both labile and recalcitrant components in the MHA fraction suggests that the stability and persistence of soil organic matter is influenced by a complex interaction of physical, chemical, and biological factors in soil. Understanding the composition and distribution of different SOM fractions can provide valuable insights into the processes that govern carbon cycling in soils, which can help inform strategies for sustainable land management and climate change mitigation.

Keywords: Soil management; ESI-FT-ICR-MS; condensed hydrocarbons; double bond equivalent; ^{13}C CPMAS NMR.

1. Introduction

Soil organic matter (SOM) content is one of the main factors influencing soil chemical, physical, and biological properties. It is the major pool of global C as it contains more than three times as much C as either the atmosphere or terrestrial vegetation (Prăvălie et al., 2021). The composition and roles of SOM have been investigated for decades, yet, its formation, transformation, and involved mechanisms are still a matter of debate (Kleber and Lehmann, 2019; Olk et al., 2019). To identify the composition of SOM in the soil ecosystem, its recalcitrance, and response to land use and climatic changes, it is necessary to identify the molecular composition of SOM fractions (Mustafa et al., 2023), especially those that cycle over suitably short time frames. Understanding SOM molecular composition is very relevant to soil in the Mediterranean basin, where climatic and pedogenic conditions and agricultural management seem to favor the loss of SOM, which results in significant environmental and financial impacts (Ferreira et al., 2022; Jones et al., 2012). Despite measures taken to conserve SOM, soils in the Mediterranean basin continue to be depleted from SOM and nutrients. Therefore, an understanding of SOM pools composition and possible transformation is necessary.

As SOM is made of different pools, isolation of specific sub-fractions of SOM that have different yet well-defined chemical characteristics and turnover rates, can allow depicting various stages of organic matter development in soil, as affected by land management (Mustafa et al., 2023; Schnitzler et al., 2007). Cao et al. (2011) introduced an integrated physical-chemical fractionation procedure to sequentially separate the light fraction of soil organic matter (LFOM), and particulate organic matter (POM), and the mobile humic acid (MHA) fraction. These SOM fractions represent different stages of SOM stabilization as the LFOM and POM fractions consist of partially decomposed plant residues, while the MHA is composed of more stabilized materials, e.g., humates. Results have shown that the humic fractions contributed disproportionately to the aromatic portion in the ^{13}C NMR spectrum of the whole SOM, while the LFOM and POM contributed to the aliphatic portion (Cao et al., 2011), suggesting that the joint use of these fractions can better describe whole SOM than can either a humic, stabilized SOM, approach or the LFOM/POM alone. Identify the molecular composition of pools representing different stage of SOM ca help identify management practices to prevent or minimize SOM depletion.

The ^{13}C NMR spectroscopy has been widely applied to characterize SOM composition in solid phases (Berns and Knicker, 2014; Mustafa et al., 2022) and has been applied to LFOM (Wang et al., 2012), POM

(Yeasmin et al., 2020), and MHA fractions (Cao et al., 2011). These studies showed that LFOM and POM were strongly aliphatic, while in contrast the MHA contained more carboxyl and aromatic functional groups. Another advanced technique, electrospray ionization Fourier transform ion cyclotron resonance mass spectrometry (ESI-FT-ICR-MS), has attracted attention for SOM characterization due to its ultrahigh mass resolution and accuracy at the molecular level (Fox et al., 2017; Kaplan et al., 2016). The FT-ICR-MS is a sophisticated characterization tool for assigning molecular formulae to thousands of individual peaks that can be detected in the mass spectrum of complex mixtures (Sleighter and Hatcher, 2011). The FT-ICR-MS has been mainly used for dissolved organic matter from aqueous environments, however, it is increasingly used to characterize soil extracts (Fernández et al., 2008; Ohno et al., 2010; Seifert et al., 2016) and humic substances (Ikeya et al., 2015, 2013) where soil humic acids (HAs) showed molecular formulae with H/C and O/C ratios similar to condensed hydrocarbons. However, only the study by Ohno et al. (2010) used FT-ICR-MS to characterize the MHA, comparing its chemical nature to those of water-extractable organic C from plants and soils. In that study, the MHA were enriched in lipid and condensed aromatic components but depleted in lignin-like compounds, whereas the aqueous plant and soil extracts contained more diverse mixtures of lipid-, protein-, carbohydrate-, and lignin-like compounds.

To our knowledge, little previous work has presented molecular-level characterization of a suit of SOM fraction that represents progressive stages of SOM stabilization in Mediterranean soils. Our work utilized the FT-ICR-MS to elucidate the molecular composition and likely transformations of three different SOM pools sequentially extracted from the same soil sample. We hypothesized that the LFOM and POM share some compositional similarities (Abdelrahman et al., 2016; Cao et al., 2011), whereas the MHA will be compositionally different. To verify the hypothesis, the objective of this work was to identify the molecular compositions of the LFOM, POM, and MHA, using the combination of ^{13}C CPMAS NMR and FT-ICR-MS to gain better insights into their chemical characteristics and possible transformations. Comparing the chemical characteristics with the progression from the physically isolated LFOM and POM to the mineral-bound MHA fraction allows a better understanding of changes in molecular composition of SOM at different stages and provide insights into which stages of SOM may be more compositionally vulnerable under different land management practices or environmental conditions. Understanding the chemical characteristics and distribution of different SOM fractions, physically extracted vs. mineral-bound, can help inform strategies for sustainable land management and carbon sequestration.

2. Materials and Methods

2.1. Site description and sampling

Soil samples were collected from two experimental field trials (Foggia and Metaponto) at different locations in the South of Italy (41°27′35″ N and 15°30′18″ E; 40°24′25″ N and 16°48′24″ E). The soils were Vertisols, specifically Typic Calcixererts (Soil Survey Staff 2014) derived from alluvium with silt and clay texture.

The cultivation history of both soils was a rotation of lentil (*Lens culinaris*) and wheat (*Triticum* sps.). In 2009, the experimental fields were converted to organic management, having fertilization treatments for different types of organic fertilizers, with three field replicates. Annual fertilization was applied to provide 100 kg N ha^{-1} to each wheat crop, or 13.1 kg P_2O_5 ha^{-1} to each lentil crop. This study focuses on compost and organo-mineral fertilizer treatments, as the common practice in Mediterranean management. In the organo-mineral fertilizer, the N component was collagen-based while the P component was collagen- and ground rock phosphate-based, and both were applied to provide the required N or P to the designated crop.

Soils were sampled after harvest where each soil sample was a composite of three cores each with three field replicates, air-dried, ground to pass through a 2-mm sieve, and then stored for subsequent analyses. Sampling depth was set to the 0–30 cm as a representative depth for field crops, the tillage and rootzone depth, and contains significant proportion of SOM, with contributions of both surface (e.g., crop residues) and root-derived organic matter inputs. More information about soils, field trials, fertilizers, and sampling are provided elsewhere (Abdelrahman et al., 2016).

2.2. SOM extraction and characterization

Soils samples (total of 48 samples representing 2 site, 2 fertilization, 2 crops, 2 sampling time, 3 replicates) were sequentially extracted for the LFOM (> 2000 µm), 500–53 µm POM, and MHA fractions. Extraction of the LFOM and POM fractions was performed with modification of the procedure by Cao et al. (2011), as described by Abdelrahman et al. (2016). The LFOM was separated by density (1.60 g mL^{-1}) using Na polytungstate followed by dispersion in Na metaphosphate and wet sieving separation of the 500–53 µm POM. The remaining silt + clay size particles were dried overnight and then used for the MHA extraction through overnight shaking in 0.25 M NaOH under an N_2 atmosphere, followed by decantation and

acidification of the supernatant to pH 1.0 using 2.0 M HCl. The humic fraction precipitates were separated through centrifugation and then cleansed of soil contaminants through re-solubilization in KOH and re-precipitation by HCl, followed by dialysis for three days in successively weaker HCl solutions and then deionized water (Mao et al., 2008). Finally, the MHA samples were lyophilized. Each field replicate was extracted separately for the SOM fractions. Averaged across both sites and both fertilizer treatments, the LFOM, POM, and MHA fractions contained 331, 307, and 442 g C kg^{-1} fraction and 18, 24, and 36 g N kg^{-1} fraction, respectively (Abdelrahman et al., 2017, 2016).

2.3. ^{13}C Cross-Polarization Magic-Angle Spinning (CPMAS) NMR

Due to the reported similarities (Abdelrahman et al., 2017, 2016) in the same fraction among different sites/treatments, only four samples of each fraction representing sites/treatments were characterized using ^{13}C CPMAS NMR. Spectra were obtained at a ^{13}C resonance frequency of 75.4 MHz on a 7.05 T Varian INOVA™ Unity (Varian Inc., Palo Alto, CA, USA). An HX Apex probe was used with a stator holding 6 mm diameter cylindrical zirconia Pencil® rotors with Vespel® drive tips. Samples were spun at 8000 ± 3 Hz at 22°C. The spectra were collected with a sweep width of 25 kHz and an acquisition time of 20 ms. The optimal contact time and recycle delay for the cross-polarization experiment were determined in preliminary experiments to be 1 ms and 5 s, respectively. During cross-polarization, the ^{1}H radio frequency (RF) field strength was set to 47.0 kHz and the ^{13}C RF field strength to 41.1 kHz. To compensate for inhomogeneities of the Hartmann-Hahn condition, an ascending ramp of 15.3 kHz on the ^{1}H-RF field was used (Berns and Conte, 2011). Proton decoupling was done using a SPINAL sequence with a ^{1}H field strength of 50.4 kHz, a phase of 4.5°, and a pulse length of 12 µs.

The free induction decays were recorded using VnmrJ (Version 1.1 RevisionD, Varian Inc., Palo Alto, CA, USA) and processed by Mestre-C (Version 4.9.9.9, Mestrelab Research, Santiago de Compostela, Spain). Fourier transformation was carried out with an exponential filter function with a line broadening (LB) of 25–50 Hz. Baseline correction was done using the manual baseline correction function of Mestre-C. The ^{13}C chemical shifts are reported relative to tetramethylsilane (=0 ppm) using adamantane as an external reference. The relative intensities of the regions were determined using the integration routine of the MestReC software. When spinning sidebands (ssb) were present, the relative intensities were corrected for the ssb as described in Berns and Conte (2011). The NMR spectra were divided into seven regions:

aliphatic (45–0 ppm), N-alkyl and methoxy (64–45 ppm), O-alkyl (90–64 ppm), di-O-alkyl (108–90 ppm), aromatics (161–108 ppm), COO/N–C=O (190–161 ppm), and ketones and aldehydes (215–190 ppm). Aliphaticity [Aliphatic C peak area (0–110 ppm)]100/[Total peak area (0–160 ppm)] and aromaticity [Aromatic C peak area (110–160 ppm)]100/[Total peak area (0–160 ppm)] of samples were calculated according to González Pérez et al. (2004).

2.4. Molecular characterization using FT-ICR-MS

Due to the reported similarities (Abdelrahman et al., 2017, 2016) in the same fraction among different sites/treatments, only four samples of each fraction representing sites/treatments were dissolved in an adequate amount of methanol in an ultrasonic bath under heat without further cleanup steps to prevent further sample loss (especially of more polar compounds) that commonly occurs during solid phase extraction. These methanol solutions were introduced by flow injection with a syringe pump at 8 µl/min into the FT-ICR-MS (LTQ-FT Ultra, ThermoFisher Scientific), equipped with an electrospray ionization (ESI) source and a 7 T superconducting magnet. Negative ion mode was utilized to prevent the dual detection of protonated and sodiated [$(M+H)^+$ and $(M+Na)^+$] ions that occur in positive ion mode.

All samples were analyzed consecutively during one day (and repeated the next day with comparable results) under the following conditions: spray voltage/capillary voltage/tube lens 2.9 kV/-50 V/-130 V, respectively; sheath-gas 3 arb, without aux-gas or sweep gas; transfer capillary 275°C; mass range 200–1000 Da. To prevent sample carry-over, flushing of the spray capillary was done first with an isopropanol-methylene chloride-chloroform mixture, followed by 10–20 fold with pure methanol. Prior to and between analyses, blanks were analyzed to exclude any memory effect in the form of a DOM pattern.

Detailed information on external and internal calibration can be found in the Supplementary Information. Peaks at several randomly selected consecutive recalibrated masses (odd and corresponding even nominal masses) were first characterized manually in order to confirm the actual mass accuracy and to determine the proper constraints in the formula assignment program (in house-developed Scilab routines). This test showed that the most intense peaks were mainly CHO peaks. Therefore, the number of heteroatoms was permitted as follows: carbon, hydrogen, and oxygen were unlimited, sulfur ≤ 1, nitrogen ≤ 2, and P=0. The molecular formula rules outlined by Stubbins et al. (2010) eliminated the vast majority of duplicate formulae for a single peak. In the cases where duplicate formulae existed (only 0.1–1.3% of the peaks), the formula

196 extension approach (Kujawinski and Behn, 2006) was utilized, where the formula chosen was that which
197 fell into a CH_2 homologous series.

198 Once molecular formulae had been assigned, various visualization diagrams were plotted. The van
199 Krevelen diagram plots the elemental ratios of H/C and O/C of the formulae, where this alignment can be
200 representative of a biochemical compound class. Kendrick mass defect (KMD) analysis separates
201 components that have similar skeletal formulae yet different quantities of a specific functional group (Ikeya
202 et al., 2015). CH_2 and COO are two common repeating units conventionally used during KMD analysis. To
203 calculate the KMD for the CH_2 group, its Kendrick mass (KM) is first calculated, leading to calculation of
204 its KMD value through the following equations (Ikeya et al., 2015):

205 $$KM\ (CH_2) = (\text{calculated mass}) \times [(\text{nominal mass of } CH_2) / (\text{exact mass of } CH_2)] \quad (1)$$

206 $$KMD\ (CH_2) = KM(CH_2) - [\text{nominal } KM(CH_2)] \quad (2)$$

207 Formulae of the same family, for example the members of an alkylation series, have the same Kendrick
208 mass defect but different nominal Kendrick masses and therefore are positioned along a horizontal line in
209 the Kendrick (CH_2) plot. Horizontal lines of different Kendrick mass defects correspond to formulae of
210 different composition, such as degrees of saturation or heteroatom content.

211 Double bond equivalent (DBE) is calculated as the sum of the number of ring structures plus the number
212 of double bonds per molecular structure, described as $C_cH_hN_nO_oS_sP_p$ (Ikeya et al., 2015), by the following
213 equation:

214 $$DBE = c - h/2 + n/2 + p/2 + 1 \quad (3)$$

215 As described by Koch and Dittmar (2006), aliphatic compounds have DBE/C<0.3 and H/C>1, and a
216 modified aromaticity index, AI_{mod}, can be used to distinguish aromatic (AI_{mod} 0.5–0.67) from condensed
217 aromatic ($AI_{mod} \geq 0.67$) entities.

218

219 **3. Results and Discussion**

220 **3.1. ^{13}C CPMAS NMR of SOM fractions**

221 The ^{13}C CPMAS NMR spectra of the LFOM fractions (Fig. S1A, Supplementary Information) were
222 dominated by the signal at 72 ppm (O-alkyl) and the N, O-substituted alkyl structures in general (108-90,
223 90-64 and 64-45 ppm). The largest signal around 72 ppm corresponds to the chemical shift of C-OH groups,
224 mostly found in carbohydrates, but also in lignin side chains. The sharp signal at 105 ppm originates from

di-O-alkyl bridges in polymeric carbohydrate chains. These chemical structures are found in cellulose, hemicellulose, starch, pectin, and lignin, though the latter usually contributes the least. The NMR spectrum of the LFOM hence confirmed the nature of the LFOM as partially decomposed plant material (Gregorich et al., 2006). The signal at 72 ppm was also the strongest signal in the spectra of the POM fractions (Fig. S1B, Supplementary Information), but the overall N,O-substituted alkyl regions (108-90, 90-64 and 64-45 ppm) were greatly reduced. This relative reduction of the carbohydrate regions indicates a slightly more advanced state of decomposition of the POM fraction compared to the LFOM fraction.

Fig. 1

The MHA spectra (Fig. S1C, Supplementary Information) were characterized by a very large and broad signal centered at 130 ppm indicating aromatic and/or unsaturated C. The aromatic region (161-108 ppm) encompassed 46–49% of the total spectral area in the MHA fraction from the Foggia plots and the unsubstituted aliphatic compounds (45–0 ppm) accounted for around 15% (Table S1, Supplementary Information). Despite the reported similarities (Abdelrahman et al., 2017, 2016) in the same fraction among different sites/treatments, significant observations are discussed. In fact, the MHA from the Metaponto plots also displayed significantly higher presence of aromatic compounds (31–32%) compared to the LFOM and POM fractions, while the relative amounts of the unsubstituted aliphatic region (45-0 ppm) were around 26–27%. Aromatic and unsubstituted aliphatic compounds require larger amounts of oxygen and energy to be metabolized and degraded by microorganisms and hence tend to accumulate in soil. In combination with the strongly reduced carbohydrate regions, the MHA spectra are consistent with stabilized C fractions (Sonsri et al., 2022). As the three fractions were isolated sequentially from the same sample, we postulate that these fractions represent a continuum of organic matter stabilization in soil.

The chemical compositions of each fraction at each site were not remarkably different between the compost and fertilizer treatments. Similarly, the spectra of LFOM and POM fractions from each fertilizer treatment did not differ notably between the two field sites. Only the MHA fraction differed visibly between the two sites. Comparison of the relative signal intensities (Table S1, Fig. S2, Supplementary Information) showed that in both treatments the MHA fraction were significantly enriched in aromatic compounds (161-108 ppm) at the Foggia site, while at the Metaponto site it showed significantly higher contents of substituted and unsubstituted aliphatics (45-0, 64-45, and 90-64 ppm). It was not expected that the chemical compositions of the fractions are not affected by fertilization, especially as the LFOM and POM fractions of

the compost treatments were expected to display significantly higher signals in the carbohydrate region stemming from degraded plant material. However, the collagen-base (i.e., protein-base) of the fertilizer probably generated similar signals, as signals from amino acids also fall within this region. Nevertheless, as fractions were extracted through flotation and wet sieving, compounds soluble in aqueous solutions (i.e., containing hydrophilic polar groups) are removed and hence part of the SOM is not recovered.

3.2. SOM molecular composition revealed by FT-ICR-MS

3.2.1. General spectral characteristics of SOM

Similar to the observations for the CPMAS NMR spectra, the FT-ICR-MS (data not shown) were fairly similar within each fraction for the different sites and compost/fertilizer treatments. For all LFOM samples, most of the peaks were detected in the *m*/*z* range of 500–650 Da. Some signals with high magnitude [>40% of the base (i.e., largest) peak in each spectrum] were observed at nominal masses 507, 509, 511, 535, and 537. These peaks corresponded to long-chain dicarboxylic acid formulae with predominantly aliphatic character (e.g., $C_{32}H_{64}O_4$, H/C=2.0, O/C=0.125). The POM spectra were mainly in the *m*/*z* range of 400–800 Da, with some signals having higher magnitudes at 250–300 Da. Peaks in the MHA spectra were detected mostly in the *m/z* ranges of 370–440 and 480–700 Da. For the POM and MHA samples, high magnitude peak clusters were detected at nominal masses 704, 819, and 935. These peaks possibly originated from triply charged Na polytungstate that had been used to separate the POM but remained in the POM and subsequently extracted MHA fraction, despite multiple washing steps. These peaks, as well as other high mass defect peaks of inorganic origin due to possible incomplete de-salting (Sleighter and Hatcher, 2011), were manually deleted from the peak lists.

Due to the presence of salt peaks and the inherent similarities among the spectra for each fraction type, only peaks that were present in all samples of the same fractional type were analyzed further. By doing so, comparisons between the LFOM, POM, and MHA fractions were more reliable, since sample preparation and instrumental reproducibility were ensured by removing peaks that were only detected in 1–3 samples of the same fractional type.

3.2.2. van Krevelen plots of SOM fractions

A conceptual van Krevelen diagram depicting the associated regions is given in Fig. S3 (Supplementary

Information). From the molecular formulae assigned to the common peaks detected in all samples of the same fraction for sites/treatments, van Krevelen diagrams were constructed (Fig. 2a), which are colored according to their heteroatom content. Table 1 summarizes the averaged mass spectral characteristics (O/C, H/C, DBE, modified aromaticity index: AI_{mod}), as well as the percentages of formulae that fall into various categories (%CHO, %CHON, %CHOS, aliphatic vs. aromatic). The CHO compounds (black points in Figs. 2–4) were by far the most abundant components, accounting for 90–92% of all formulae in the LFOM and POM and about 83% of the formulae in the MHA (Table 1). Formulae containing S and N (blue and red points, respectively, in Figs. 2–4) were less abundant and most fell into the aliphatic category with high H/C.

The van Krevelen diagrams for the compiled formulas of the LFOM and POM fractions (Fig. 2a) were similar, having average O/C and H/C values of 0.24–0.26 and 1.69–1.72, respectively. Most of these formulae fell into the lipid-like (H/C 1.5–2.0, O/C 0–0.3) aliphatic region, as previously reported (Hockaday et al., 2009; Ohno et al., 2010; Sleighter and Hatcher, 2008). In contrast, the MHA molecular formulae were grouped in two clearly separated ranges: the lipid-like region and the condensed hydrocarbon region (H/C 0.2–0.7, O/C 0.0–0.67) often categorized as black carbon. Carbohydrates (especially those without carboxylic groups), which have high O/C and high H/C, generally cannot adequately compete for a charge during the ESI process of complex mixtures and are therefore not detected in the mass spectra here, or those reported elsewhere (Hockaday et al., 2009; Ohno et al., 2010). The van Krevelen plot of the MHA fraction reported by Ohno et al. (2010) also showed molecular formulae that clustered mostly in the two separate regions of lipid-like and condensed hydrocarbon spaces, with some also aligning in the lignin-like central region (H/C 0.7–1.5, O/C 0.1–0.67). The present MHA fraction showed scarce formula assignments in the lignin space. This lack of lignin assignments in the MHA might be related to the fully aerobic soil conditions, which would promote lignin oxidation (DiDonato et al., 2016). Nevertheless, Ge et al. (2022) found that river dissolved organic matter associated with cropland inputs was dominated by lignin-like species with higher O/C and lower H/C ratio. This indicate that the lignin-like species may have different pathways of transport and transformation in different environmental contexts. Having essentially no molecular formulae assigned to the lignin space in the MHA plot (Fig. 2a) indicated that the MHA had progressed beyond initial humification status, which is in line with Ohno et al. (2010) who concluded that formation of the MHA is marked by a decrease in lignin components and an increase in condensed aromatic components. Consistently, (Olk et al., 2006) used ^{13}C CPMAS NMR to find the MHA, from paddy rice soils, enriched in phenolic

lignin residues, suggesting incomplete decomposition, as phenolic lignin compounds are normally oxidized and degraded during the humification processes (DiDonato et al., 2016). Although condensed aromatic components are less susceptible to degradation and can contribute to long-term carbon sequestration in soil, adopting conservative practices, such as cover crop and reduced tillage, that prevent the oxidation of relatively less recalcitrant components such as lignin residues can contribute to SOM accumulation.

D'Andrilli et al. (2015) introduced the molecular lability boundary (MLB) to differentiate between molecular constituents of natural organic matter that vary in intrinsic lability. The MLB is set at H/C=1.5, so formulae having H/C>1.5 are defined as more labile compounds (lipid-like and aliphatic region) while formulae having H/C<1.5 are defined as more recalcitrant materials in the aromatic and condensed aromatic regions. The proportion of formulae in the labile region appear most pronounced in the POM (93% of formulae have H/C$\geq$1.5) similar to LFOM (89% of formulae have H/C$\geq$1.5) but in contrast to MHA (74% of formulae have H/C$\geq$1.5), as shown in Table 1 and Fig. 2a. Intrinsic biochemical lability of compounds can differ from their degradability in soils, likely depending on their location within the soil matrix, their strength of binding to the soil mineral surfaces or within SOM, and the presence of specific microbial enzymes. Yet, D'Andrilli et al. (2015) provided some validation for the MLB by associating relative labilities estimated through this process for dissolved organic carbon samples with their degradation rates during weekly incubations.

Figure 2b shows the relationship between H/C ratios and *m*/*z* for the common formulas of the SOM fractions. The molecular formulae with H/C ratios greater than 1.5 were distributed throughout the mass range of 250–800 Da in all analyzed fractions. This suggests that these compounds are likely to be present in a variety of SOM molecules with different mass ranges. In contrast, molecular formulae with low H/C ratios (0.3–0.6), which are indicative of condensed aromatics, were only observed within the m/z range of 400–800 Da. The limited distribution of condensed aromatics in the higher mass range may reflect their relative recalcitrance to degradation. Furthermore, the presence of labile components in the MHA, within the m/z range of 250–400 Da, suggests its relative susceptibility to decomposition by soil microorganisms. The combined presence of both recalcitrant and labile components implies that the MHA contribution to long-term carbon sequestration in soil, depends on practices that promote SOM conservation. Overall, these results suggest that the composition of MHA is complex and dynamic, with a diverse range of molecular formulae and susceptibility to microbial degradation.

Table 1

Fig. 2

3.2.3. The Kendrick mass analysis

The Kendrick mass analysis is useful for grouping compounds with similar structural characteristics, such as the presence of functional groups or the degree of unsaturation, which can facilitate the identification of compounds that are structurally related and may have similar properties, such as solubility, reactivity, or stability. The LFOM and POM fractions clearly differed from the MHA fraction in the relationships between the KMD (CH_2) and the nominal Kendrick mass (Fig. 3a). The LFOM and POM compounds were situated in one wide band extending to higher KMD values, which corresponds to the high H/C aliphatic compounds shown in the van Krevelen diagrams (Fig. 2a). This wide band was also present in the MHA fraction, but a second, narrower band having considerably lower KMD (0.1–0.5) was distinctly separate, correlating to the condensed aromatics at low H/C in the van Krevelen diagram. Formulae that aligned at the same KMD value across the mass range are indicative of an alkylation series. Formulae with high KMD (i.e., high H/C) have longer CH_2 homologous series, i.e., more CH2 groups in their alkylation series, covering a wider mass range. The lower KMD (i.e., low H/C) formulae have fewer components in each homologous series, because condensed aromatic ring systems have less opportunity for CH_2 expansions. The KMD findings indicate that the MHA fraction is composed of a complex mixture of both aliphatic and aromatic compounds with different degrees of unsaturation. This complexity, reflecting both both recalcitrant and labile components, highlights the importance of management practices that promote SOM conservation for long-term carbon sequestration.

Fig. 3

3.2.4. The distribution of double bond equivalent (DBE) values

The DBE describes the degree of unsaturation and help predicting the properties and reactivity of organic compounds. As shown in Fig. 3b, the DBE values increased progressing from the LFOM and POM (average DBE of approximately 6, with values as high as 25) to the MHA (average DBE of 9, with values up to 33). The vast majority of molecular formulae in the LFOM and POM had DBE $\leq$11, which held true across the

entire mass range. The MHA fraction showed two clearly different DBE regions of molecular formulae, whether graphed against *m*/*z*, H/C, or O/C (Figs. 3–4), similar to the Inogashira humic acid as reported by Ikeya et al. (2012). The MHA region with lower DBE values (mostly ≤12 across the *m*/*z* range of 300–800 Da with higher H/C of 1.4–2.1, Fig. 4a) is characteristic of aliphatic lipid-like components (Ikeya et al., 2012), consistent with those found in the LFOM and POM. The second region – found exclusively in the MHA – exhibited extremely high DBE values (from 17 at *m*/*z* 400 Da up to 33 at *m*/*z* 800 Da), low H/C values (0.33–0.60), and higher O/C values (0.35–0.65, Fig. 4b). This set of traits indicates components having yet higher degrees of microbially driven oxidation and condensation, corresponding to a higher number of DBE than those reported elsewhere (Ikeya et al., 2015)

Fig. 4

Exemplary structures of specific formulae with exceptionally high DBE values in the MHA fraction are provided in Fig. 5, in order to illustrate the types of structures that could give rise to such DBE values. It should be noted that many other structural isomers are also possible. In general, the low H content dictates that these structures be condensed polycyclic aromatic hydrocarbons (PAHs) with abundant double bonds and rings. Simultaneously, abundant oxygen – often as much as hydrogen – is also incorporated, accounting for the high O/C ratios. These presumptions are not incongruent with the NMR results, as we expect these condensed PAHs to represent only a subset of all inherent organic molecules in the MHA fraction.

Fig. 5

Presuming that in general carbonyl compounds (as in Fig. 5c) as a reactive species should be rather unstable in soil, and therefore seldom found, and above all, their ionization efficiencies in negative ion mode are lower than carboxylic groups, we hypothesize that these high DBE formulae are oxygenated condensed PAHs bearing mostly hydroxyl- and carboxylic side groups as postulated in Figs. 5a, b. These condense PAHs shall be consistent with the significant presence of carboxyl C in the NMR spectrum (Fig. 1) and of aromatic C in both the NMR spectrum and the van Krevelen diagram (Fig. 2a) of the MHA. Such C contents between 59 and 65% in the examples given in Fig. 5 are similar to those of humic substances, where the humic acids commonly contain >55% C.

The DBE–H/C plots (Fig. 4a) suggest the sequential evolution of SOM fractions from the LFOM and POM fractions derived from plant and physically uncomplexed SOM fractions to the mineral-bound MHA fraction. The molecular formulae of the LFOM and POM were mainly in the aliphatic region (DBE <10,

H/C 1.5–2), while the MHA had a greater proportion of its molecular formulae with distinctly higher DBE and lower H/C, which are characteristic of condensed PAHs. The various DBE plots together with the NMR spectra, the van Krevelen plots, and their derived calculations, collectively demonstrate a continuum of increasingly degraded/stabilized composition from the LFOM/POM to the MHA. This continuum is consistent with the proposed increasing degree of decomposition from the LFOM/POM to the MHA, as also demonstrated by the carbohydrate compositions of these fractions (Abdelrahman et al. 2016). These findings indicate that the MHA is composed of both plant-derived and microbially-derived components, reflecting the dynamic nature of SOM composition.

The presence of condensed aromatic C in the MHA and SOM may have multiple sources, as suggested by the literature. These sources include precursors of smaller condensed aromatic structures (2–5 rings) such as polynuclear quinones produced by fungi, as hypothesized earlier (e.g., Ikeya et al., 2015). A second potential source is charred-like plant materials that were subjected to degradation and oxidation processes within the soils (Abdelrahman et al., 2018). A third possible precursor is possibly produced from the transformation of lignin in the presence of hydroxyl radicals (Ikeya et al., 2015; Waggoner et al., 2015). The availability of lignin residues in soil and the absence of lignin signals in the van Krevelen plots of MHA underscores the potential of this mechanism for creating condensed aromatic C, but our data are not suited to distinguish between the three potential sources. Previous studies provided ample evidence that condensed aromatic C structures in humic fractions such as the MHA are not created artificially during the alkaline extraction and are instead naturally occurring species (Olk et al., 2019).

3.3. NMR vs. FT-ICR-MS perspectives

The FT-ICR-MS and NMR analyses were used to study the molecular composition of successively isolated SOM fractions, and the results revealed differences in the molecular compositions of the successively isolated SOM fractions. According to the molecular formulae signatures, the composition of the LFOM, POM, and the MHA can be characterized as follows: i) aliphatic substances were common in all three fractions and were most abundant in the LFOM and POM; ii) molecular formulae assigned to the lignin range were practically negligible; and iii) molecular formulae assigned to condensed aromatic hydrocarbons were characteristic of only the MHA. Hence, the MHA contained both labile fragments with H/C >1.5, as well as more condensed aromatic compounds with *m*/*z* >400 and DBE >17 (>4 rings), which suggest

recalcitrant SOM substances.

However, solid state NMR analysis revealed that the LFOM was primarily composed of carbohydrates, which aligns with previous NMR studies conducted on the LFOM (Cao et al., 2011, Abdelrahman et al., 2016), in contrast to the FT-ICR-MS characterization that identified the LFOM as mostly lipid and aliphatic. This discrepancy is observed as large carbohydrate polymers have low solubility and limited ionization efficiencies in negative ion mode ESI, due to their relatively lower ionic nature when compared to components containing carboxylic acid groups. Another potential difference between the methods is that unsubstituted aromatic C is more visible in NMR than in ESI-FT-ICR-MS, due to its nonpolar nature. Advanced forms of ^{13}C NMR are considered to be a more quantitative measure of all C forms within SOM (Mao et al., 2017), while the qualitative ESI prefers ionic polar compounds and is only semi-quantitative at best. Yet the FT-ICR-MS more precisely characterized the components that it could detect, providing individual formulae instead of the broad classes of functionality that NMR provides.

The absence of a lignin signature in the MHA fraction suggests that lignin may have been further degraded or synthesized to the condensed aromatic hydrocarbons observed in the MHA. This observation is consistent with the decomposition/humification continuum of soil C, and indicates that the intrinsic chemical nature of inputted materials may indeed affect their respective cycling rates, which contradicts the belief that SOM cycling is solely dictated by microbial access.

4. Conclusions and implications

This study investigated the molecular composition of different soil organic matter (SOM) fractions and differentiated them based on their molecular characteristics. The LFOM and POM fractions were found to contain mainly aliphatic substances, while lignin-like formulae were negligible, and condensed aromatic hydrocarbons were exclusive to the MHA fraction. The MHA fraction exhibited both labile fragments with H/C >1.5 and condensed aromatic compounds with m/z >400 and DBE >17, implying the presence of recalcitrant SOM substances. The coexistence of labile and recalcitrant components in the MHA highlights the importance of adopting practices that result in physical protection of this SOM pool in aggregates and organo-mineral complexes to promote long-term carbon sequestration. This study sheds light on the molecular composition and possible transformations of labile SOM fractions in Mediterranean arable soils and emphasizes the significance of understanding SOM compositional changes in response to environmental

and agronomic conditions. The findings reported here offers potential implications into agriculture and environment as the identification of specific SOM fractions, that are more prone to decomposition/stabilization or prime SOM decomposition under different environmental conditions, can help to inform strategies for enhancing carbon sequestration in agricultural soils by tailoring practices that promote the accumulation of recalcitrant SOM fractions. Further research is necessary to determine if the findings of this study are specific to the sampled locations or applicable to other agroecosystems and environmental settings.

Acknowledgement: Authors thank Roland Bol, IBG-3, Forschungszentrum Jülich (FZJ), for his comments on the first draft and Bernhard Steffen (FZJ, retired) for his support in the development and expansion of the evaluation program for FT-ICR-MS data. Authors thanks the anonymous reviewers for their constructive comments and suggestions on the manuscript.

References

Abdelrahman, H., Cocozza, C., Olk, D.C., Ventrella, D., Miano, T., 2017. Carbohydrates and Amino Compounds as Short-Term Indicators of Soil Management. Clean - Soil, Air, Water 45. https://doi.org/10.1002/clen.201600076

Abdelrahman, H., Hofmann, D., Berns, A.E.A.E., Meyer, N., Bol, R., Borchard, N., 2018. Historical charcoal additions alter water extractable, particulate and bulk soil C composition and stabilization. J. Plant Nutr. Soil Sci. 181, 809–817. https://doi.org/10.1002/jpln.201800261

Abdelrahman, H.M., Olk, D.C., Dinnes, D., Ventrella, D., Miano, T., Cocozza, C., 2016. Occurrence and abundance of carbohydrates and amino compounds in sequentially extracted labile soil organic matter fractions. J. Soils Sediments 16, 2375–2384. https://doi.org/10.1007/s11368-016-1437-y

Berns, A.E., Conte, P., 2011. Effect of ramp size and sample spinning speed on CPMAS 13C NMR spectra of soil organic matter. Org. Geochem. 42, 926–935.

Berns, A.E., Knicker, H., 2014. Soil Organic Matter. eMagRes 3, 43–54. https://doi.org/10.1002/9780470034590.EMRSTM1345

Cao, X., Olk, D.C., Chappell, M., Cambardella, C.A., Miller, L.F., Mao, J., 2011. Solid-State NMR Analysis of Soil Organic Matter Fractions from Integrated Physical–Chemical Extraction. Soil Sci. Soc. Am. J. 75, 1374–1384. https://doi.org/10.2136/SSSAJ2010.0382

D'Andrilli, J., Cooper, W.T., Foreman, C.M., Marshall, A.G., 2015. An ultrahigh-resolution mass spectrometry index to estimate natural organic matter lability. Rapid Commun. Mass Spectrom. 29, 2385–2401.

DiDonato, N., Chen, H., Waggoner, D., Hatcher, P.G., 2016. Potential origin and formation for molecular components of humic acids in soils. Geochim. Cosmochim. Acta 178, 210–222. https://doi.org/10.1016/J.GCA.2016.01.013

Fernández, J.M., Hockaday, W.C., Plaza, C., Polo, A., Hatcher, P.G., 2008. Effects of long-term soil amendment with sewage sludges on soil humic acid thermal and molecular properties. Chemosphere 73, 1838–1844.

Ferreira, C.S.S., Seifollahi-Aghmiuni, S., Destouni, G., Ghajarnia, N., Kalantari, Z., 2022. Soil degradation in the European Mediterranean region: Processes, status and consequences. Sci. Total Environ. 805, 150106. https://doi.org/10.1016/J.SCITOTENV.2021.150106

Fox, P.M., Nico, P.S., Tfaily, M.M., Heckman, K., Davis, J.A., 2017. Characterization of natural organic matter in low-carbon sediments: Extraction and analytical approaches. Org. Geochem. 114, 12–22.

Ge, J., Qi, Y., Li, C., Ma, J., Yi, Y., Hu, Q., Mostofa, K.M.G., Volmer, D.A., Li, S.L., 2022. Fluorescence and molecular signatures of dissolved organic matter to monitor and assess its multiple sources from a polluted river in the farming-pastoral ecotone of northern China. Sci. Total Environ. 837, 154575. https://doi.org/10.1016/J.SCITOTENV.2022.154575

González Pérez, M., Martin-Neto, L., Saab, S.C., Novotny, E.H., Milori, D.M.B.P., Bagnato, V.S., Colnago, L.A., Melo, W.J., Knicker, H., 2004. Characterization of humic acids from a Brazilian Oxisol under different tillage systems by EPR, 13C NMR, FTIR and fluorescence spectroscopy. Geoderma 118, 181–190. https://doi.org/10.1016/S0016-7061(03)00192-7

Gregorich, E.G., Beare, M.H., McKim, U.F., Skjemstad, J.O., 2006. Chemical and Biological Characteristics of Physically Uncomplexed Organic Matter. Soil Sci. Soc. Am. J. 70, 975–985.

Hockaday, W.C., Purcell, J.M., Marshall, A.G., Baldock, J.A., Hatcher, P.G., 2009. Electrospray and photoionization mass spectrometry for the characterization of organic matter in natural waters: A qualitative assessment. Limnol. Oceanogr. Methods 7. https://doi.org/10.4319/lom.2009.7.81

Ikeya, K., Sleighter, R.L., Hatcher, P.G., Watanabe, A., 2015. Characterization of the chemical composition of soil humic acids using Fourier transform ion cyclotron resonance mass spectrometry. Geochim. Cosmochim. Acta 153, 169–182. https://doi.org/10.1016/J.GCA.2015.01.002

Ikeya, K., Sleighter, R.L., Hatcher, P.G., Watanabe, A., 2013. Fourier transform ion cyclotron resonance mass spectrometric analysis of the green fraction of soil humic acids. Rapid Commun. Mass Spectrom. 27, 2559–2568.

Ikeya, K., Sleighter, R.L., Hatcher, P.G., Watanabe, A., 2012. Compositional features of Japanese Humic Substances Society standard soil humic and fulvic acids by Fourier transform ion cyclotron resonance mass spectrometry and X-ray diffraction profile analysis. Humic Subst. Res. 9.

Jones, A., Panagos, P., Barcelo, S., Bouraoui, F., Bosco, C., Dewitte, O., Gardi, C., Hervás, J., Hiederer, R., Jeffery, S., Montanarella, L., Penizek, V., Toth, G., Van Den Eeckhaut, M., Van Liedekerke, M., Verheijen, F.G.A., Yigini, Y., Erhard, M., Lukewille, A., Petersen, J., Marmo, L., Olazabal, C., Strassburger, T., Viestova, E., 2012. State of Soil in Europe. https://doi.org/10.2788/77361

Kaplan, D.I., Xu, C., Huang, S., Lin, Y., Tolić, N., Roscioli-Johnson, K.M., Santschi, P.H., Jaffé, P.R., 2016. Unique Organic Matter and Microbial Properties in the Rhizosphere of a Wetland Soil. Environ. Sci. Technol. 50, 4169–4177.

Kleber, M., Lehmann, J., 2019. Humic Substances Extracted by Alkali Are Invalid Proxies for the Dynamics and

Functions of Organic Matter in Terrestrial and Aquatic Ecosystems. J. Environ. Qual. 48, 207–216.
Koch, B.P., Dittmar, T., 2006. From mass to structure: An aromaticity index for high-resolution mass data of natural organic matter. Rapid Commun. Mass Spectrom. 20. https://doi.org/10.1002/rcm.2386
Kujawinski, E.B., Behn, M.D., 2006. Automated analysis of electrospray ionization fourier transform ion cyclotron resonance mass spectra of natural organic matter. Anal. Chem. 78. https://doi.org/10.1021/ac0600306
Mao, J., Cao, X., Olk, D.C., Chu, W., Schmidt-Rohr, K., 2017. Advanced solid-state NMR spectroscopy of natural organic matter, Progress in Nuclear Magnetic Resonance Spectroscopy. Pergamon.
Mao, J., Olk, D.C., Fang, X., He, Z., Schmidt-Rohr, K., 2008. Influence of animal manure application on the chemical structures of soil organic matter as investigated by advanced solid-state NMR and FT-IR spectroscopy. Geoderma 146, 353–362.
Mustafa, A., Frouz, J., Naveed, M., Ping, Z., Nan, S., Minggang, X., Núñez-Delgado, A., 2022. Stability of soil organic carbon under long-term fertilization: Results from 13C NMR analysis and laboratory incubation. Environ. Res. 205, 112476. https://doi.org/10.1016/J.ENVRES.2021.112476
Mustafa, A., Saeed, Q., Karimi Nezhad, M.T., Nan, S., Hongjun, G., Ping, Z., Naveed, M., Minggang, X., Nú nez-Delgado, A., 2023. Physically separated soil organic matter pools as indicators of carbon and nitrogen change under long-term fertilization in a Chinese Mollisol. Environ. Res. 216, 114626. https://doi.org/10.1016/J.ENVRES.2022.114626
Ohno, T., He, Z., Sleighter, R.L., Honeycutt, C.W., Hatcher, P.G., 2010. Ultrahigh Resolution Mass Spectrometry and Indicator Species Analysis to Identify Marker Components of Soil- and Plant Biomass-Derived Organic Matter Fractions. Environ. Sci. Technol. 44, 8594–8600. https://doi.org/10.1021/ES101089T
Olk, D.C., Bloom, P.R., Perdue, E.M., McKnight, D.M., Chen, Y., Farenhorst, A., Senesi, N., Chin, Y.-P., Schmitt-Kopplin, P., Hertkorn, N., Harir, M., 2019. Environmental and Agricultural Relevance of Humic Fractions Extracted by Alkali from Soils and Natural Waters. J. Environ. Qual. 48, 217–232. https://doi.org/10.2134/JEQ2019.02.0041
Olk, D.C., Cassman, K.G., Schmidt-Rohr, K., Anders, M.M., Mao, J.D., Deenik, J.L., 2006. Chemical stabilization of soil organic nitrogen by phenolic lignin residues in anaerobic agroecosystems. Soil Biol. Biochem. 38, 3303–3312.
Prăvălie, R., Nita, I.A., Patriche, C., Niculiță, M., Birsan, M.V., Roșca, B., Bandoc, G., 2021. Global changes in soil organic carbon and implications for land degradation neutrality and climate stability. Environ. Res. 201, 111580. https://doi.org/10.1016/J.ENVRES.2021.111580
Schnitzler, F., Lavorenti, A., Berns, A.E., Drewes, N., Vereecken, H., Burauel, P., 2007. The influence of maize residues on the mobility and binding of benazolin: Investigating physically extracted soil fractions. Environ. Pollut. 147, 4–13.
Seifert, A.G., Roth, V.N., Dittmar, T., Gleixner, G., Breuer, L., Houska, T., Marxsen, J., 2016. Comparing molecular composition of dissolved organic matter in soil and stream water: Influence of land use and chemical characteristics 571, 142–152.
Sleighter, R.L., Hatcher, P.G., 2011. Fourier Transform Mass Spectrometry for the Molecular Level Characterization of Natural Organic Matter: Instrument Capabilities, Applications, and Limitations. Fourier Transform. - Approach to Sci. Princ. https://doi.org/10.5772/15959
Sleighter, R.L., Hatcher, P.G., 2008. Molecular characterization of dissolved organic matter (DOM) along a river to ocean transect of the lower Chesapeake Bay by ultrahigh resolution electrospray ionization Fourier transform ion cyclotron resonance mass spectrometry. Mar. Chem. 110, 140–152. https://doi.org/10.1016/J.MARCHEM.2008.04.008
Soil Survey Staff (2014) Keys to Soil Taxonomy, 12th ed. USDA-Natural Resources Conservation Service, Washington, DC.
Sonsri, K., Naruse, H., Watanabe, A., 2022. Mechanisms controlling the stabilization of soil organic matter in agricultural soils as amended with contrasting organic amendments: Insights based on physical fractionation coupled with 13C NMR spectroscopy. Sci. Total Environ. 825, 153853. https://doi.org/10.1016/J.SCITOTENV.2022.153853
Stubbins, A., Spencer, R.G.M.M., Chen, H., Hatcher, P.G., Mopper, K., Hernes, P.J., Mwamba, V.L., Mangangu, A.M., Wabakanghanzi, J.N., Six, J., 2010. Illuminated darkness: Molecular signatures of Congo River dissolved organic matter and its photochemical alteration as revealed by ultrahigh precision mass spectrometry. Limnol. Oceanogr. 55, 1467–1477.
Waggoner, D.C., Chen, H., Willoughby, A.S., Hatcher, P.G., 2015. Formation of black carbon-like and alicyclic aliphatic compounds by hydroxyl radical initiated degradation of lignin. Org. Geochem. 82, 69–76.
Wang, Q., Zhang, L., Zhang, J., Shen, Q., Ran, W., Huang, Q., 2012. Effects of compost on the chemical composition of SOM in density and aggregate fractions from rice-wheat cropping systems as shown by solid-state 13C-NMR spectroscopy. J. Plant Nutr. Soil Sci. 175. https://doi.org/10.1002/jpln.201100350
Yeasmin, S., Singh, B., Smernik, R.J., Johnston, C.T., 2020. Effect of land use on organic matter composition in

588 density fractions of contrasting soils: A comparative study using 13C NMR and DRIFT spectroscopy. Sci.
589 Total Environ. 726, 138395. https://doi.org/10.1016/J.SCITOTENV.2020.138395
590

Figure Captions

Fig. 1. ^{13}C CPMAS NMR spectra of a) the light fraction of soil organic matter (LFOM), b) the 500–53 μm particulate organic matter (POM) fraction, and c) the mobile humic acid (MHA) fraction from the compost treated plots at the Metaponto site (arrow = center glitch).

Fig. 2. van Krevelen diagrams of the FT-ICR-MS molecular formulae that were common to all 4 site/treatment combinations for each fraction (a) and the relationship between atomic H/C and *m/z* for the common molecular formulae (b) for the light fraction of soil organic matter (LFOM), the 500–53 μm particulate organic matter (POM), and the mobile humic acid (MHA) fractions. Formulas are colored according to heteroatom content (CHO, CHON, and CHOS formulas are black, red, and blue, respectively).

Fig. 3. Kendrick mass defect analysis plots as a function of CH_2 (a) and the relationship between double bond equivalents (DBE) and *m/z* for the molecular formulae that were common to all 4 site/treatment combinations for each fraction (b) for the light fraction of soil organic matter (LFOM), the 500–53 μm particulate organic matter (POM), and the mobile humic acid (MHA) fractions. Formulas are colored according to heteroatom content (CHO, CHON, and CHOS formulas are black, red, and blue, respectively).

Fig. 4. Relationships between double bond equivalents (DBE) and H/C (a) or O/C (b) for the molecular formulae that were common to all 4 site/treatment combinations for the light fraction of soil organic matter (LFOM), the 500–53 μm particulate organic matter (POM), and the mobile humic acid (MHA) fraction. Formulas are colored according to heteroatom content (CHO, CHON, and CHOS formulas are black, red, and blue, respectively).

Fig. 5. Structure proposals to illustrate possible skeletal structures and functional groups for randomly selected formulae with varying high DBE values in the mobile humic acid (MHA) fraction.

Table 1. The number-averaged O/C, H/C, DBE, and AI_{mod} values for the molecular formulas that were common to all four site/treatment combinations for each fraction (LFOM, POM, and MHA), as well as the percentage of formulas that fall into categories based on aromaticity (aliphatic, aromatic, condensed aroamtic), heteroatom content (CHO, CHON, CHOS), and lability (calculated from the molecular lability boundary, D'Andrilli et al., 2015).

Fraction	O/C	H/C	DBE	AI_{mod}	% Aliphatic	% Aromatic	% Condensed Aromatic	% CHO	% CHON	% CHOS	% Labile
LFOM	0.24	1.69	6.2	0.09	90.7%	0.8%	0.0%	90.2%	5.8%	4.0%	88.5%
POM	0.26	1.72	5.4	0.06	94.9%	0.0%	0.0%	92.2%	2.8%	5.0%	92.9%
MHA	0.30	1.51	8.9	0.18	76.3%	0.4%	17.1%	82.8%	4.4%	12.9%	73.6%

LFOM; light fraction of soil organic matter; POM: 500–53 µm particulate organic matter; MHA: mobile humic acid; DBE: double bond equivalent; AI_{mod}: modified aromaticity index

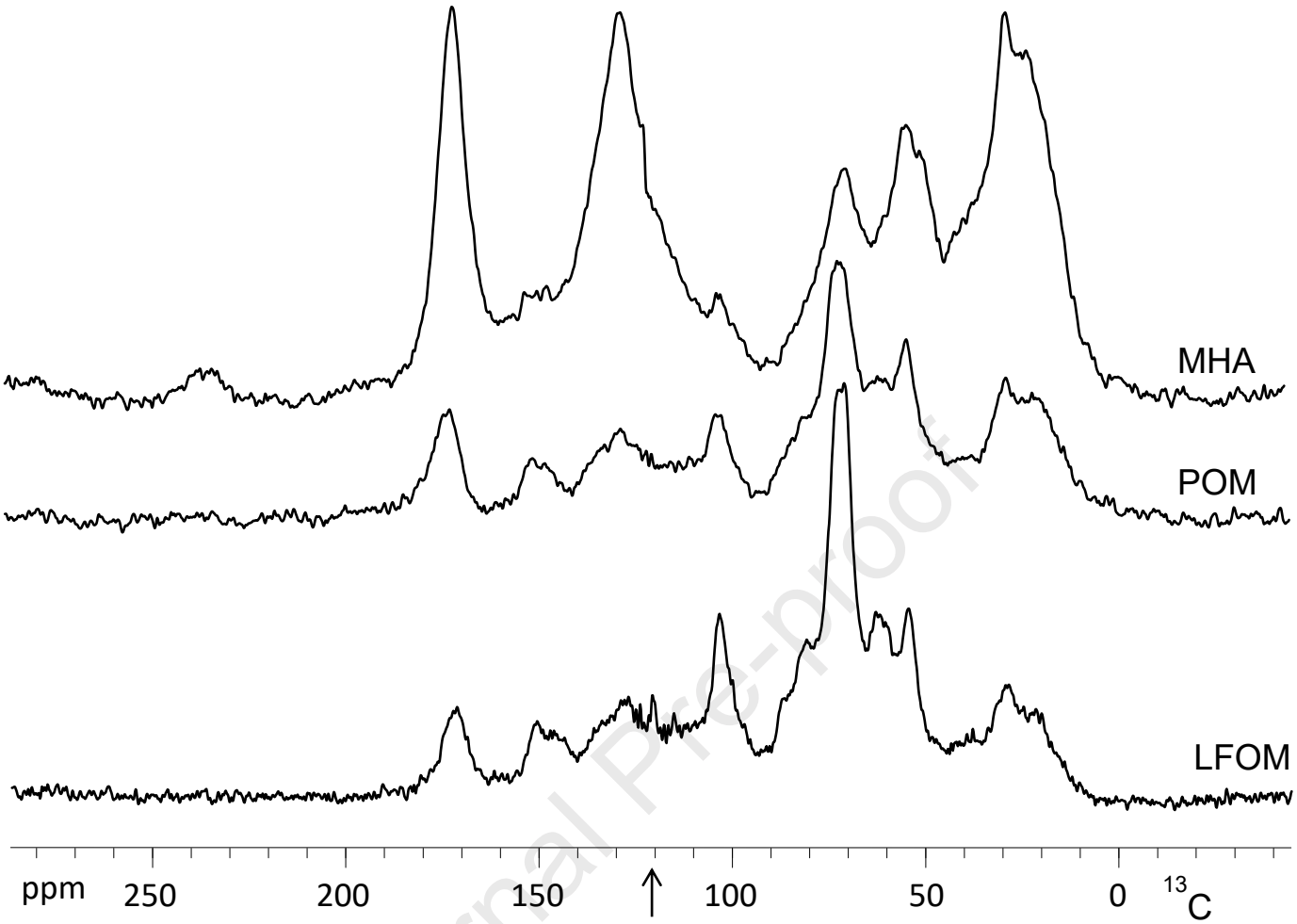

Figure 1

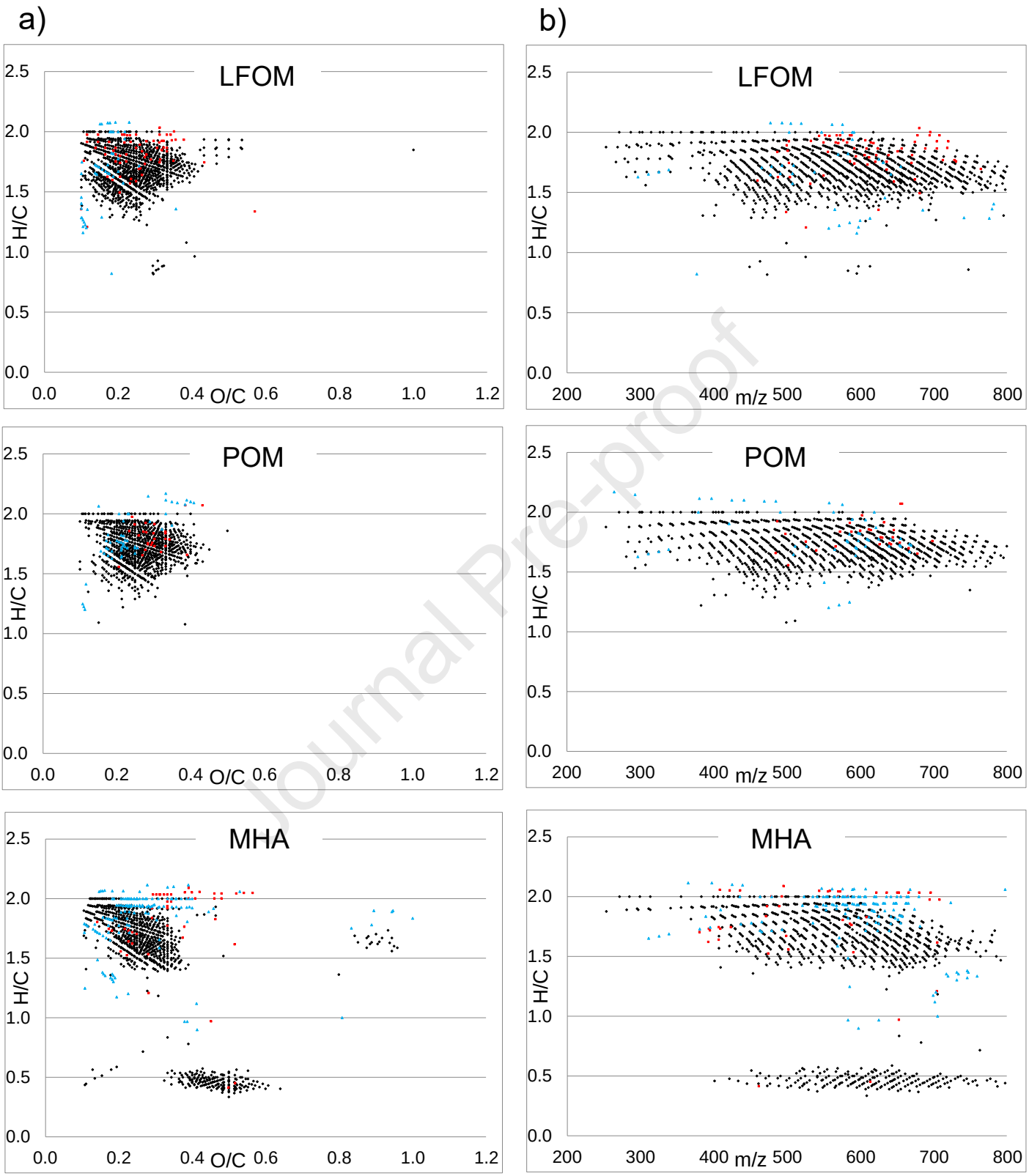

Figure 2

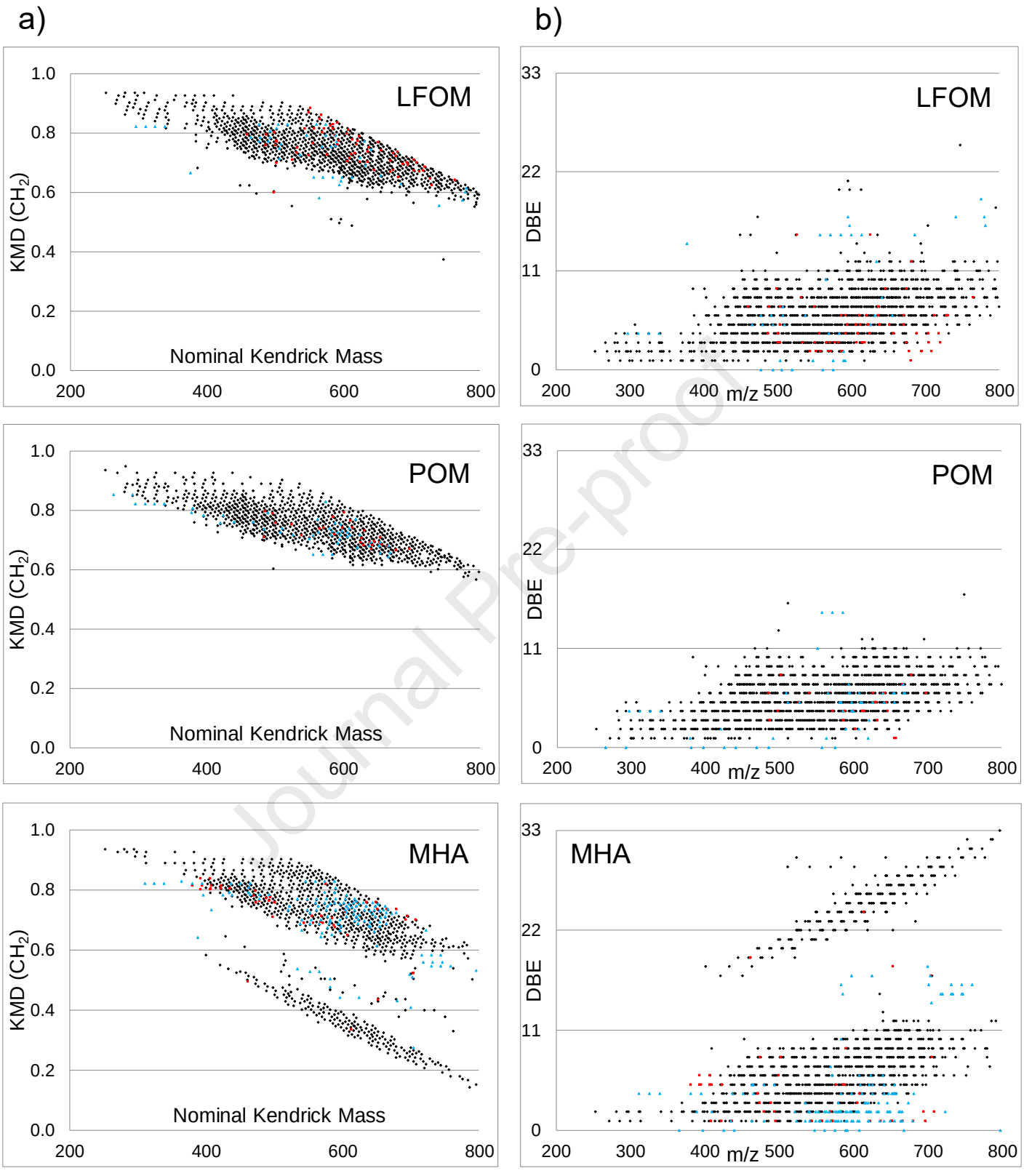

Figure 3

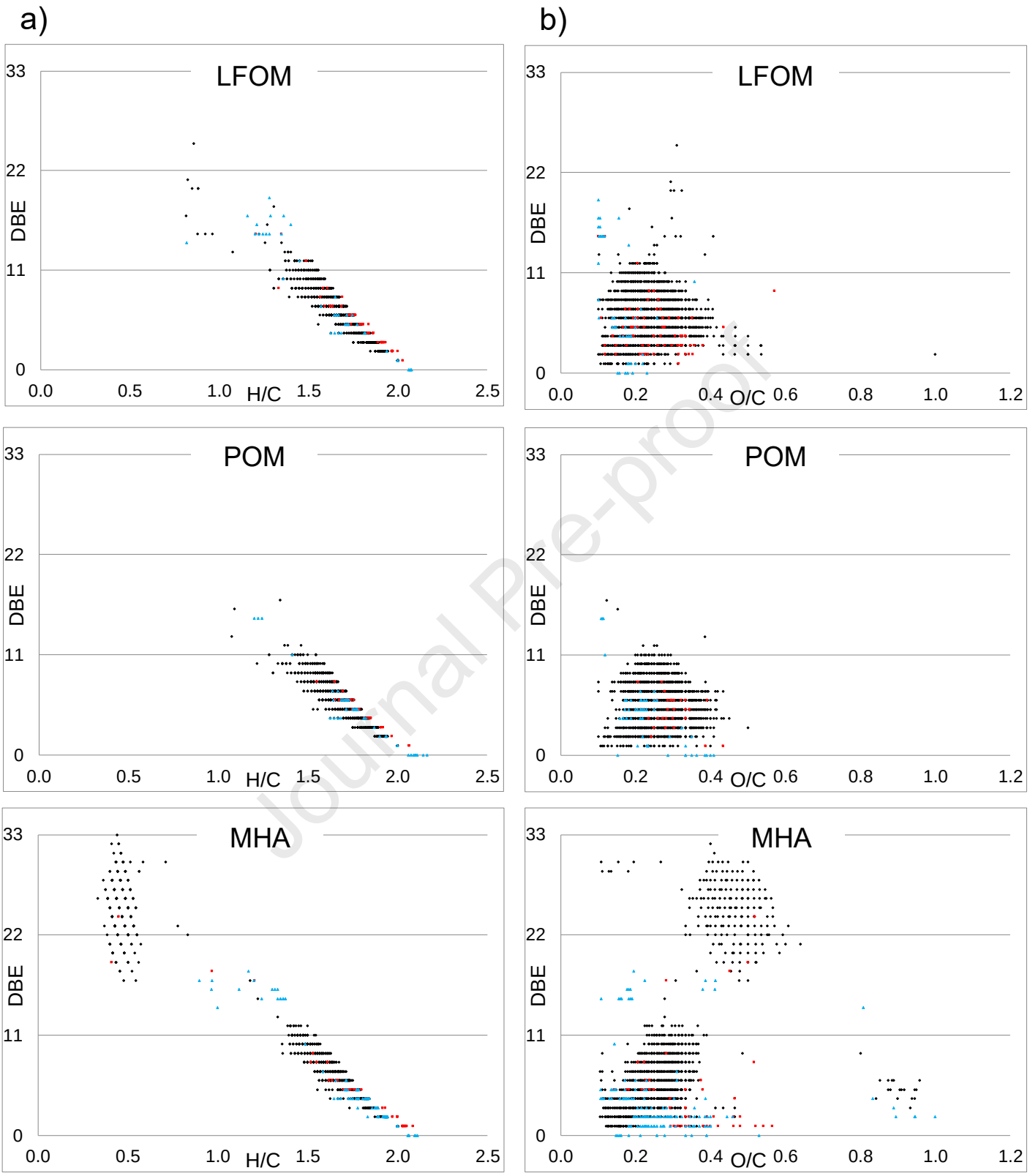

Figure 4

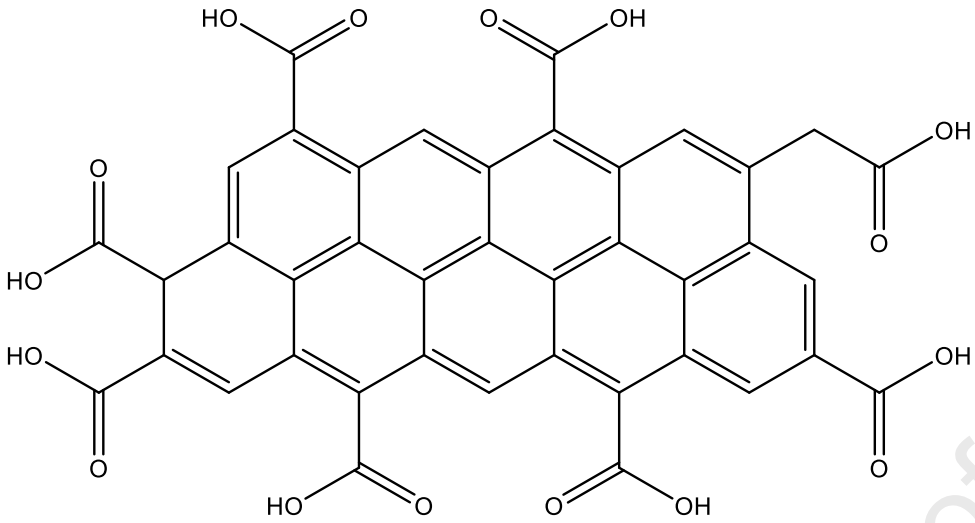

a)
$C_{40}H_{18}O_{16}$
64% C
DBE=32
H/C=0.40
O/C=0.45
753.052214 (1-)

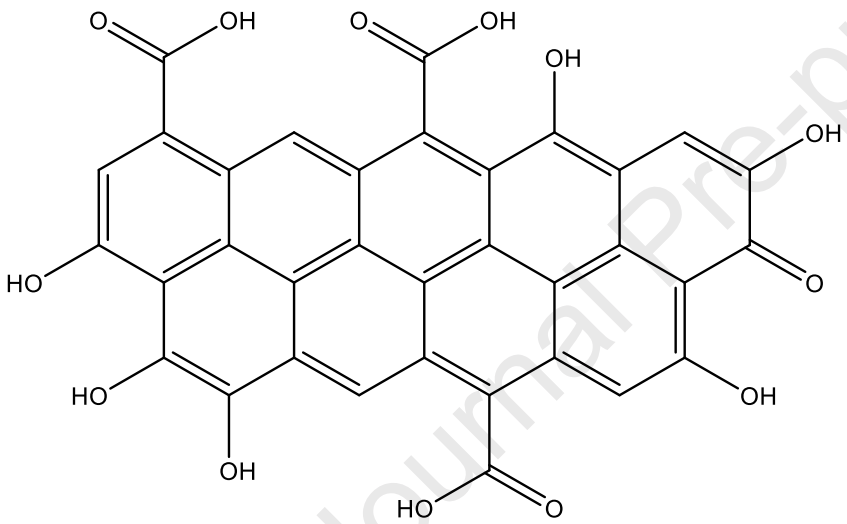

b)
$C_{34}H_{14}O_{13}$
65% C
DBE=28
H/C=0.38
O/C=0.41
629.036169 (1-)

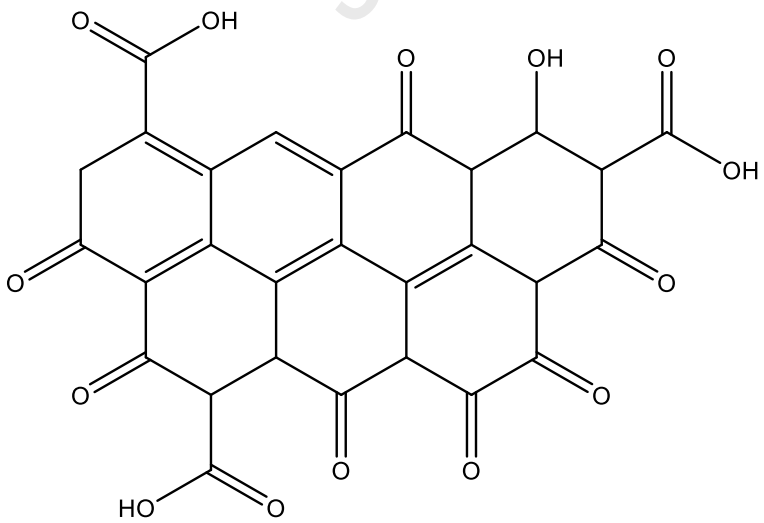

c)
$C_{28}H_{14}O_{14}$
59% C
DBE=22
H/C=0.50
O/C=0.50
573.031084 (1-)

Figure 5

Declaration of interests

☒ The authors declare that they have no known competing financial interests or personal relationships that could have appeared to influence the work reported in this paper.

☐The authors declare the following financial interests/personal relationships which may be considered as potential competing interests: